

Identification of cysteinylated transthyretin, a predictive biomarker of treatment response to partially hydrolyzed guar gum in type 2 diabetes rats, by surface-enhanced laser desorption/ionization time-of-flight mass spectrometry

Yuji Naito,^{1,*} Hiroshi Ichikawa,² Satomi Akagiri,^{1,#} Kazuhiko Uchiyama,¹ Tomohisa Takagi,¹ Osamu Handa,¹ Zenta Yasukawa,³ Makoto Tokunaga,³ Noriyuki Ishihara,³ Tsutomu Okubo,³ Jun Mukai,⁴ Makoto Ohki,⁴ Kagehiro Uchida⁴ and Toshikazu Yoshikawa¹

¹Molecular Gastroenterology and Hepatology, Kyoto Prefectural University of Medicine, 465 Kajii-cho, Kamigyo-ku, Kyoto 602-8566, Japan

²Department of Medical Life Systems, Faculty of Life and Medical Sciences, Doshisha University, 1-3 Tatara Miyakodani, Kyotanabe-shi, Kyoto 610-0321, Japan

³Nutrition Division, Taiyo Kagaku Co., Ltd., 1-3 Takaramachi, Yokkaichi, Mie 510-0844, Japan

⁴Biomarker Science Co., Ltd., 103-5 Tanaka-Monzencho, Sakyo-ku, Kyoto 540-0029, Japan

(Received 14 August, 2015; Accepted 27 August, 2015; Published online 8 December, 2015)

Recent evidence has indicated that total fiber intake is inversely related to type 2 diabetes risk. The present study aimed to investigate the effects of chronic administration of partially hydrolyzed guar gum (PHGG), a water-soluble dietary fiber, on the occurrence of diabetes and its complications, fatty liver and nephropathy. We also identified predictive serum biomarkers of treatment response to PHGG by mass spectroscopy-based proteomic analysis using Otsuka Long-Evans Tokushima Fatty (OLETF) rats, a good model of human non-insulin-dependent diabetes mellitus. In this study, at 5 weeks of age, OLETF rats and control strain Long-Evans Tokushima Otsuka (LETO) rats were fed a control diet or a high-fiber diet (5% PHGG) for 57 weeks. Body weight, food intake, oral glucose tolerance test, plasma insulin levels, and urine glucose and protein levels were regularly measured. Oral glucose tolerance tests (OGTT) and storage of serum in a deep freezer were conducted at the beginning of the experiment and every 4 weeks after overnight fasting during the experiments. PHGG treatment affected neither meal patterns nor the body weight of OLETF and LETO rats. Repeated measure analysis of variance revealed significant differences in fasting plasma glucose and plasma glucose at 2 h after OGTT between control OLETF (OLETF-C) rats and OLETF rats treated with PHGG (OLETF-F). The glucose response determined by the area under the curve of OGTT was significantly greater in OLETF-C rats than that in OLETF-F rats at 25 weeks of age. HOMA-IR, an index of insulin resistance, increased at 25 weeks of age in OLETF-C rats, while this increase was significantly inhibited in OLETF-F rats. At 62 weeks of age, PHGG treatment significantly improved hepatic steatosis as well as renal mesangial matrix accumulation in OLETF rats. To identify the risk marker for diabetes mellitus by SELDI-TOF MS, we collected sera from 21-week-old individuals. Among the 12 specific peaks that were risk marker candidates for diabetes mellitus, the *m/z* 13,720 peak was identified as that of cysteinylated transthyretin by sequencing of four tryptic peptides using tandem mass spectrometry and peak distribution around the *m/z* 13,720 peak in the SELDI-TOF spectra. In conclusion, we found that chronic treatment with PHGG improved insulin resistance, delayed the onset of diabetes, and

inhibited the development of diabetic complications, as well as identified cysteinylated transthyretin as a predictive biomarker of treatment response to PHGG in OLETF rats.

Key Words: biomarker, cysteinylation, diabetes mellitus, dietary fiber, transthyretin

Chronic diseases such as diabetes, cancer, hypertension and cardiovascular disease have become major public health issues in modern societies. The only effective means for dealing with these health issues is likely through preventive medicine. The long asymptomatic period before the onset of chronic diseases offers good opportunities for disease prevention. For example, diabetes mellitus (DM) may be preventable by avoiding high caloric diets that trigger the disease process (primary prevention) or by exercise or the intake of food factors that modulate the disease process before the onset of clinical symptoms (secondary prevention). It has been reported that several beneficial food factors,⁽¹⁾ calorie restriction,⁽²⁾ and exercise can prevent the occurrence of diabetes and/or the development of diabetic complications in diabetes animal models.⁽³⁾ Particularly, the preventive effects against diabetes have been demonstrated using several functional food factors including α -lipoic acid,⁽⁴⁾ fermented-grain food,⁽⁵⁾ vitamin E,⁽⁶⁾ and *S*-allyl cysteine.⁽⁷⁾ In these preventive studies, the Otsuka Long-Evans Tokushima Fatty (OLETF) rat is typically used as a model of spontaneous type 2 diabetes.^(8,9) The characteristics of OLETF rats include a chronic course of disease, late onset of hyperglycemia, mild obesity, fatty liver, and diabetic nephropathy. These features in OLETF rats resemble those of human type 2 diabetes.⁽⁹⁾

In planning effective disease prevention studies, sensitive and specific biomarkers that can accurately identify the at-risk popula-

*To whom correspondence should be addressed.

E-mail: ynaito@koto.kpu-m.ac.jp

[#]Present address: Department of Food Nutritional Science, Kobe Women's Junior College, 7-2, 4-chome, Minatojima-nakamachi, Chuo-ku, Kobe, Hyogo 650-0046, Japan

tion before the onset of clinical symptoms are required, particularly in human studies. Molecular profiling has rapidly become the method of choice for biomarker identification, as a large number of genes and proteins can be analyzed using high-throughput technologies. One approach involving quantitative proteomics is based on surface-enhanced laser desorption/ionization time-of-flight mass spectrometry (SELDI-TOF MS). SELDI utilizes chromatographic surfaces that retain proteins from a complex sample mixture according to their specific properties; and the molecular weights of the retained proteins are then measured by TOF MS. Using this approach, candidate biomarkers have been identified as a diagnostic markers for a number of diseases including lung cancer,⁽¹⁰⁾ hepatocellular carcinoma,⁽¹¹⁾ laryngeal squamous carcinoma,⁽¹²⁾ peripheral arterial disease,⁽¹³⁾ dementia,⁽¹⁴⁾ acute pancreatitis,⁽¹⁵⁾ and chronic obstructive pulmonary disease.⁽¹⁶⁾ Interestingly, recent studies in human have identified candidate biomarkers predictive of clinical outcome of anti-cancer drugs,⁽¹⁷⁾ infliximab,⁽¹⁸⁾ and interferon plus ribavirin therapy.⁽¹⁹⁾

In the present study, we demonstrated that chronic administration with partially hydrolyzed guar gum (PHGG), a water-soluble dietary fiber, slowed the occurrence of diabetes and inhibited the fatty liver and renal dysfunction in OLETF rats. We also identified predictive biomarkers of the treatment response to PHGG in type 2 diabetes rats using SELDI-TOF MS.

Materials and Methods

Diet preparation. The commercial PHGG preparation (Sunfiber[®]) used in this study was obtained from Taiyo Kagaku Co., Ltd. (Mie, Japan). The preparation was manufactured by treatment with guar gum using a β -endogalactomannase from a strain of *Aspergillus niger*. High-performance liquid chromatography (HPLC) analysis was used to determine that the average molecular mass of PHGG was 20,000 Da. The total dietary fiber content of PHGG was 85%, as measured using the method described by the Association of Official Agricultural Chemists.

Animal experiments and diet composition. All animal experiments and care conformed to the Guidelines of the Animal Care and Use Committee of Kyoto Prefectural University of Medicine. Four-week-old male OLETF rats ($n = 14$) and LETO rats ($n = 8$) were provided by the Tokushima Research Institute of Otsuka Pharmaceutical (Tokushima, Japan) without charge. After acclimation for 1 week by feeding a basal diet, the rats were randomly assigned to one of four dietary regimens: 1) OLETF-C ($n = 7$); OLETF rats fed control standard rat diet (CRF-1, Oriental Yeast Co., Ltd., Tokyo, Japan), 2) OLETF-F ($n = 7$); OLETF rats fed standard rat diet containing 5% PHGG, 3) LETO-C ($n = 4$); LETO rats fed control standard diet, and 4) LETO-F ($n = 4$); LETO rats fed standard rat diet containing 5% PHGG. Nutritional information of the standard diet CRF-1: metabolizable energy 359 kcal/100 g, 22.4% protein, 5.7% fat, 3.1% fiber, while that for the PHGG fiber diet: metabolizable energy 341 kcal/100 g, 21.2% protein, 5.4% fat, and 8.1% fiber. The rats were individually housed in plastic cages at $24 \pm 2^\circ\text{C}$ and at $45 \pm 5\%$ relative humidity with a 12-h/12-h light/dark cycle, and were given free access to food and water throughout the experimental period.

Body weight, oral glucose tolerance test, and insulin resistance. Food consumed was evaluated each day and body weight was evaluated every week during the experiments. Oral glucose tolerance tests (OGTT) were conducted at the beginning of the experiments and every 4 weeks after overnight fasting during the experiments. Rats were administered a 20% glucose solution (2 g/kg) and blood samples were collected from the tail vein at 0, 30, 60, and 120 min after glucose loading. Plasma glucose levels were determined using a Glutest Ace R (Sanwa Kagaku Kenkyusho Co., Ltd., Nagoya, Japan). Based on the results of OGTT, normal glucose tolerance (shown as “N” in Fig. 3b) was defined as fasting plasma glucose (FPG) <110 mg/dl

and 2 h post-glucose loading <140 mg/dl. Diabetes (“D” in Fig. 3b) was defined as FPG ≥ 126 mg/dl or 2 h post-load glucose ≥ 200 mg/dl. The remaining rats in each group were evaluated for impaired glucose tolerance (“I” in Fig. 3b), characterized by normal glucose tolerance and diabetes. The homeostasis model assessment of insulin resistance (HOMA-IR) was calculated using glucose and insulin concentrations obtained after 7 h of food withdrawal by using the following formula: fasting blood glucose (mg/dl) \times fasting insulin ($\mu\text{U/ml}$)/405. Plasma insulin levels were measured using an insulin ELISA kit (Morinaga Institute of Biological Science, Inc., Yokohama, Japan).

Serum lipids and biochemistry. Asparate 2-oxoglutarate aminotransferase, alanine 2-oxoglutarate aminotransferase, blood urea nitrogen, free cholesterol, triglyceride, non-esterified fatty acid, and LDL-cholesterol were measured using a Shimadzu CL8000 Clinical Chemistry Analyzer (Shimadzu, Ltd., Tokyo, Japan).

Evaluation of fatty liver and nephropathy. OLETF rats were sacrificed at 62 weeks of age and their livers and kidneys were fixed in 10% buffered formalin and embedded in paraffin. The paraffin-embedded tissue sections were deparaffinized in xylene, rehydrated with a series of alcohol washes, and then stained with hematoxylin-eosin (H-E) and with periodic acid-Schiff (PAS) reagent and hematoxylin to evaluate hepatic steatosis and diabetic nephropathy, respectively. In each H-E-stained section of the renal cortex, the severity of hepatic histological steatosis was assessed and the ratio of fatty lesions was calculated as fatty area/(total area-vascular area) $\times 100$ (%) using NIH Image Software and Photoshop (Adobe Systems, San Jose, CA). In each PAS-stained section of the renal cortex, 20 glomeruli cuts at the vascular pole were analyzed morphometrically. The extent of increase in the mesangial matrix was determined by the presence of PAS-positive and nuclei-free area in the mesangium; the glomerular area was also traced along the outline of the capillary loop using NIH Image Software and Photoshop. The ratio of PAS-positive mesangial area was calculated as mesangial matrix area/glomerular area $\times 100$ (%). Rats were transferred to individual metabolic cages for urine sample collection, and urine samples were collected for 24 h to measure albumin clearance; urinary albumin concentration $\times 24$ -h urine volume.

Protein profiling using SELDI-TOF MS. The samples were examined in duplicate and each replicate of samples (10 μl) was denatured by adding 20 ml of U9 buffer [50 mM Tris-HCl (pH 9.0), 9 M urea, 2% CHAPS] and then agitated at 4°C for 20 min. Denatured samples were applied to 50 ml of Q Ceramic Hyper D[®] F (Pall Corporation, Port Washington, NY) anion exchanger resin and subsequently 20 ml of U1 buffer [9-fold diluted U9 buffer containing 50 mM Tris-HCl (pH 9.0)] was added to each resin, and the samples were incubated at 4°C for 30 min. Six fractions including flow through + pH 9.0, 7.0, 5.0, 4.0, and 3.0 and organic, which were referred to as Fr1–Fr6, respectively, were collected using 50 ml of 50 mM Tris-HCl buffer (pH 9.0) containing 0.1% octyl β -D-glucopyranoside (OGP) and washed twice with 50 ml of four different buffers twice with stepwise-decreasing pH values: 50 mM HEPES-NaOH buffer (pH 7.0) with 0.1% OGP; 100 mM sodium acetate buffer (pH 5.0) containing 0.1% OGP; 100 mM sodium acetate buffer (pH 4.0) containing 0.1% OGP; 50 mM sodium citrate buffer (pH 3.0) containing 0.1% OGP. As the final step, the resin was washed twice with 50 ml of organic solution composed of 33.3% isopropanol, 16.7% acetonitrile (ACN), and 0.1% trifluoroacetic acid (TFA) to elute residual proteins.

All fractionated samples were subjected to two different types of ProteinChip[®] array (Bio-Rad, Hercules, CA), including CM10 (weak cation exchange) and IMAC30 (immobilized metal affinity capture) coupled with Cu^{2+} . The binding buffer contained 100 mM sodium acetate buffer (pH 4.0) for the CM10 arrays and 100 mM sodium phosphate buffer (pH 7.0) containing 500 mM NaCl for

the IMAC30-Cu²⁺ arrays. Aliquots (10 ml) of the fractionated samples were diluted 0-fold with the respective binding buffers and applied to ProteinChip® arrays. Both α -cyano-4-hydroxycinnamic acid and sinapinic acid (SPA) were used as an energy-absorbing molecules (EAMs). An aliquot of 1 ml of EAM (50% saturated concentration in 50% ACN, 0.5% TFA) was applied twice to the prepared arrays. After sample denaturation to apply EAM, the laboratory automation system Biomek 2000® (Beckman Instruments Co., Coulter, CA) was employed to analyze the samples.

All arrays were analyzed using a Protein Biological System IIC ProteinChip® reader (Bio-Rad). The high mass setting was set to 100 kDa and the focus mass was set to 6.5 kDa. The arrays were analyzed under two different conditions when using SPA as an EAM, the high mass setting was set to 200 kDa, and the focus mass was set to 20 kDa in addition to the above settings. Mass spectrometric profiles were generated by averaging 130 laser shots under optimized analysis conditions based on maximum protein peak yield.

Purification and identification of protein biomarkers.

The protein biomarker of *m/z* 14,720 was purified and identified as follows. A strong anion-exchange column, the HiTrap™ Q HP 1 ml (GE Healthcare Bio-Sciences, Pittsburgh, PA), was equilibrated with U1 buffer. A 1.5-ml aliquot of normal rat serum (SHIMIZU Laboratory Supplies Co., Kyoto, Japan) was denatured by adding 450 μ l U9 buffer and applied to the column. The column was washed with 5 ml of 50 mM Tris-HCl (pH 9.0) buffer and subsequently washed with 5 ml of 50 mM sodium acetate (pH 5.0) buffer and an additional 5 ml of 0.50 mM sodium citrate buffer (pH 3.0). The column was washed with 33.3% isopropanol, 16.7% ACN, and 0.1% TFA to elute the retained proteins to obtain the target fraction.

The obtained fraction was subjected to 15–20% tricine SDS-PAGE under non-reducing conditions. Gels were stained with coomassie brilliant blue (CBB) G-250. To confirm that the target protein was isolated, the protein bands were passively eluted with 50% formic acid, 25% ACN, and 15% isopropanol from the polyacrylamide gel matrix followed by SELDI-TOF MS analysis. To identify the proteins, corresponding bands were analyzed by peptide mass fingerprinting (PMF) according to a previous study.⁽²⁰⁾ TOF MS spectra of tryptic peptides were acquired using a 4700 Proteomics Analyzer (Applied Biosystems, Foster City, CA) and intense peaks in TOF MS spectra were analyzed in tandem mass spectrometry mode to obtain MS/MS spectra. Obtained TOF MS and MS/MS spectra were analyzed using the mass values of monoisotopic peaks for searches (MASCOT: <http://www.matrixscience.com/>) against the SWISS-Prot database.

Statistics. For each outcome measure in animal models, one-way analysis of variance (ANOVA) was performed (Prism 6 for Mac OS X, GraphPad Software, Inc., San Diego, CA). Significant main effects ($p < 0.05$) between the OLETF-C and OLETF-F groups at each week of age were followed up with student's *t* test. Values are reported as the mean \pm SE, and a *p* value < 0.05 indicated a statistically significant difference.

Data processing and analysis for protein profiles were performed using Ciphergen Express™ 3.0 (Bio-Rad). Baseline subtraction was performed and then the processed spectra were normalized to the total ion current. Detected peaks were identified in the peak cluster list and *p* values were calculated using the Mann-Whitney *U* test to compare normalized peak intensities between given sample groups. In this study, a *p* value less than 0.1 was regarded as statistically significant because of the small sample size ($n = 4$).

Results

Effect of PHGG on food intake and body weight in OLETF and LETO rats. As shown in Fig. 1a, OLETF-C rats were hyperphagic relative to LETO-C, with 40–50% more daily food

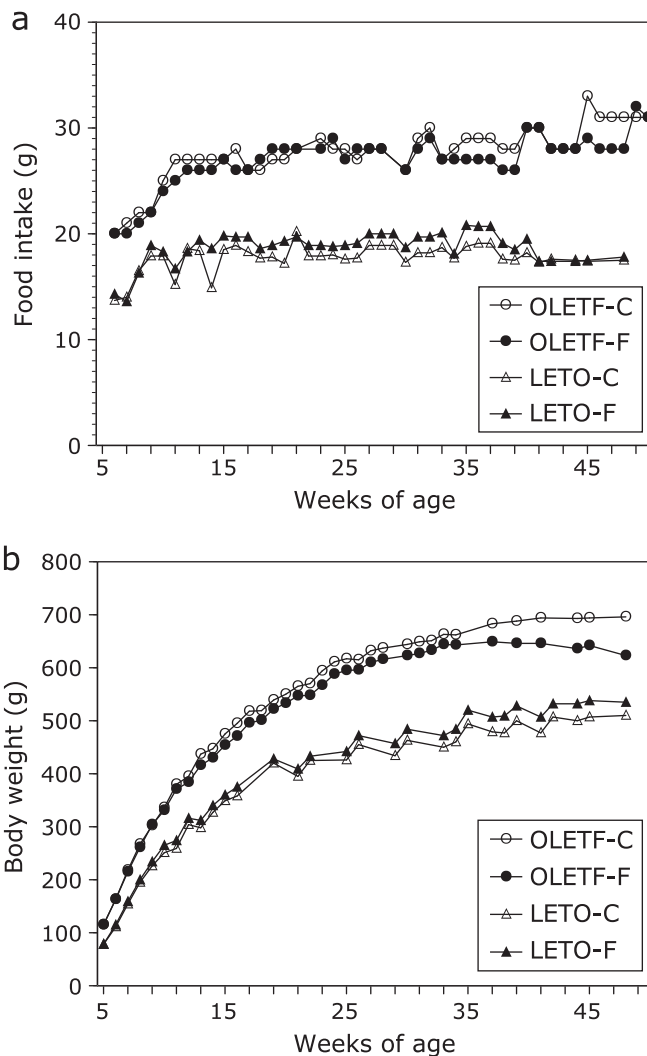


Fig. 1. Weekly food intake (a) and body weight (b) in OLETF and LETO rats. Values are means ($n = 7$ and 4 animals in OLETF groups and LETO groups, respectively). OLETF was significantly different from LETO group, but PHGG affected neither body weight nor food intake in OLETF and LETO rats. OLETF-C, OLETF rats treated with control diet; OLETF-F, OLETF rats treated with high-fiber (PHGG) diet; LETO-C, LETO rats treated with control diet; LETO-F, LETO rats treated with high-fiber (PHGG) diet.

intake over the period of 6–62 weeks of age. There was no significant effect of PHGG treatment on the meal patterns of both OLETF and LETO rats. We found that the body weights of the two groups in OLETF rats were significantly higher than those of LETO controls (Fig. 1b). PHGG treatment affected neither the body weight nor the phenotype of rats fed a control diet during the experiment.

Effect of PHGG on plasma levels of glucose in OLETF and LETO rats. As shown in Fig. 2a, the fasting plasma glucose levels in OLETF-C rats were similar to those in LETO-C rats until 21 weeks of age, and gradually increased from 25 weeks of age. Plasma glucose levels 2 h after OGTT in OLETF-C rats also gradually increased from 19 weeks of age. Repeated measure ANOVA revealed significant differences both in plasma glucose levels for fasting and 2 h after OGTT between OLETF-C and OLETF-F groups ($F = 6.365$, $p < 0.05$ for fasting plasma glucose, $F = 18.9$, $p < 0.001$ for plasma glucose 2 h after OGTT).

Glucose responses to an OGTT and HOMA-IR are shown in

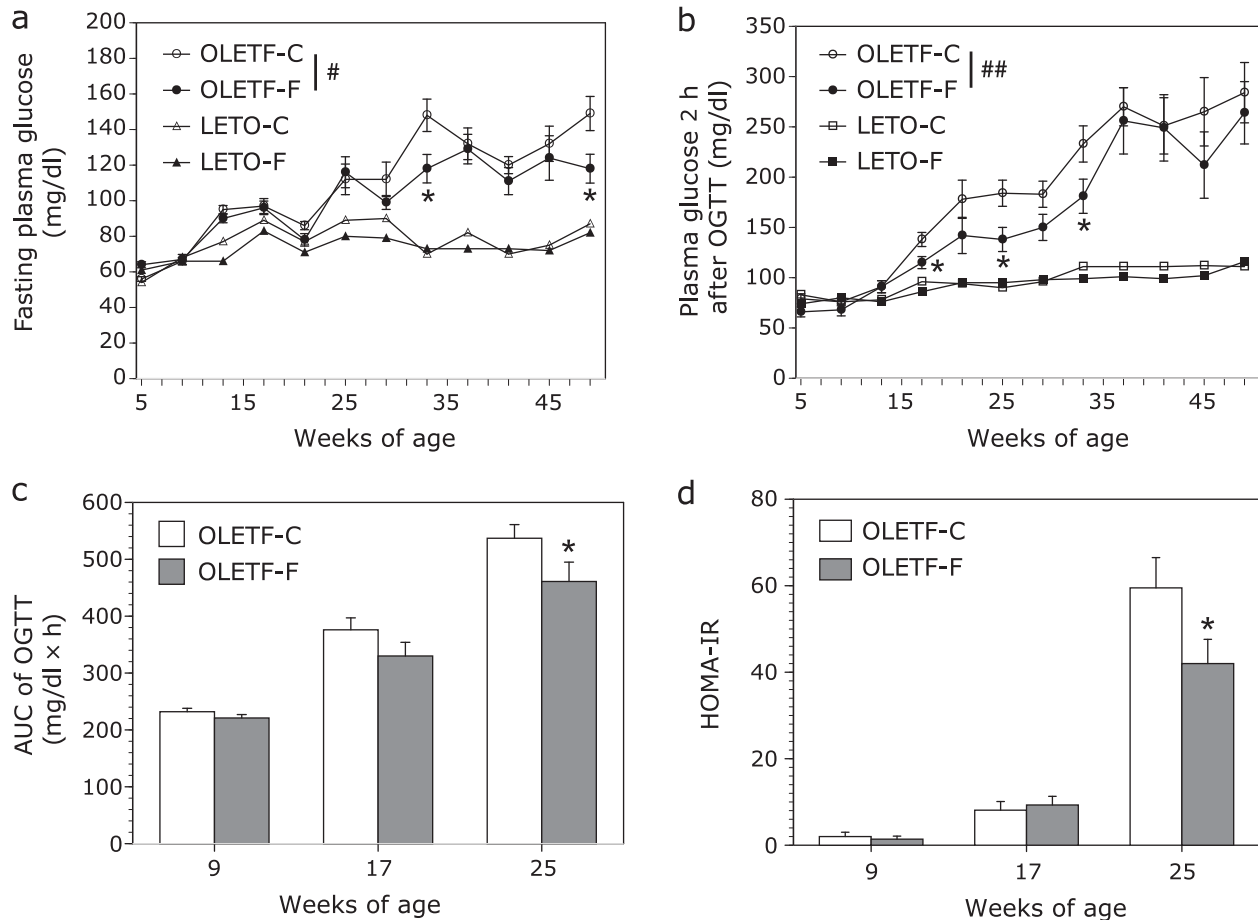


Fig. 2. Weekly fasting plasma glucose (a) and plasma glucose 2 h after OGTT (b) in OLETF and LETO rats, and the area under the curve (AUC) of glucose (c) and HOMA-IR (d) in OLETF rats. Repeated measure ANOVA revealed significant differences between OLETF-C and OLETF-F groups ($*p<0.05$, and $##p<0.001$). $*p<0.05$ vs OLETF-C rats by student t test. OLETF-C, OLETF rats treated with control diet; OLETF-F, OLETF rats treated with high-fiber (PHGG) diet; LETO-C, LETO rats treated with control diet; LETO-F, LETO rats treated with high-fiber (PHGG) diet.

Fig. 2c and d, respectively. The area under the curve (AUC) of glucose and HOMA-IR in OLETF-C rats increased at 25 weeks of age, and these increased values were significantly ($p<0.05$) inhibited by treatment with PHGG.

Effect of PHGG on the onset of impaired glucose tolerance (IGT) and diabetic (DM) patterns determined by OGTT.

The median onset of IGT/DM was 21 weeks of age and 25 weeks of age in the OLETF-C and OLETF-F groups, respectively. A comparison of the incidence curves is shown in Fig. 3a; there was a significance difference between the OLETF-C and OLETF-F groups ($p = 0.03$, Log-rank test). Fig. 3b showed each result in the OGTT in OLETF-C and OLETF-F rats during the experiment.

Effects of PHGG on fatty liver and renal dysfunction in OLETF rats. Histological analysis showed the severe fatty infiltration at the periphery of the central vein in the liver of OLETF-C rats at 62 weeks of age compared with LETO rats, and treatment with PHGG clearly improved hepatic steatosis in OLETF rats (Fig. 4a). Consistent with the histological findings, PHGG significantly ($p<0.05$) reduced the ratio of fatty lesions in the liver of OLETF rats (Fig. 4b).

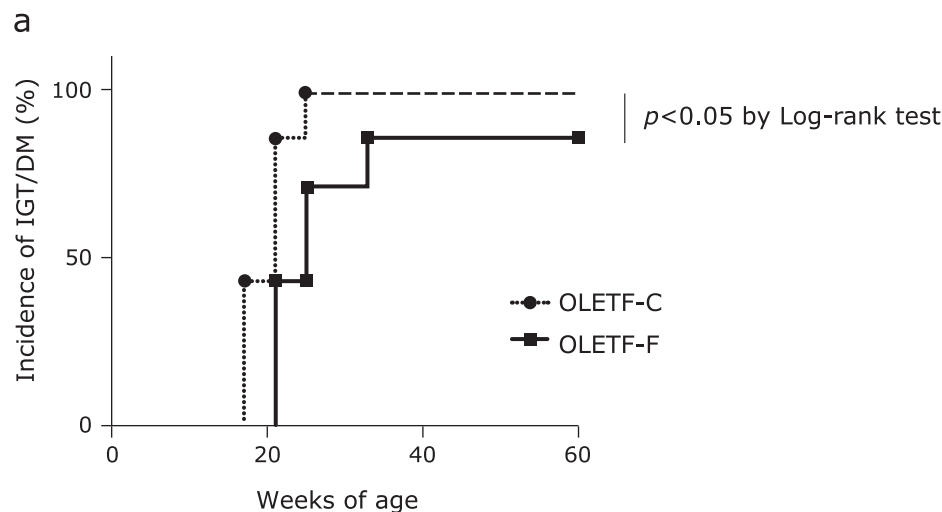
The glomerular appearance in OLETF-C rats at 62 weeks of age showed accelerated mesangial expansion characterized by an increase in PAS-positive mesangial matrix area relative to that observed in LETO-C rats. Chronic treatment with PHGG attenuated mesangial matrix accumulation and significantly inhibited the increase in relative mesangial area calculated as

the mesangial area/total glomerular area ratio (Fig. 5a and b). In addition, albumin levels in the urine of OLETF-C rats increased compared with those in LETO-C rats at 42, 53, and 60 weeks of age. These increases in urinary albumin of OLETF-C rats were significantly inhibited in OLETF-F rats at 53 and 60 weeks of age (Fig. 5c).

Effects of PHGG on serum biochemistry in OLETF rats.

As shown in Table 1, there were no significant differences in serum biochemical parameters between OLETF-C and OLETF-F rats at 62 weeks of age, except for non-esterified fatty acid, which significantly ($p<0.05$) decreased in OLETF-F rats compared to that in OLETF-C rats.

Discovery of the risk marker for diabetes mellitus by SELDI analysis. We hypothesized that the blood collected just before the onset of DM should clearly reflect the risk of DM. Thus, based on the results of OGTT (Fig. 3b), serum samples subjected for proteomics analysis by SELDI-TOF MS were selected. To identify risk markers for DM, we examined sera collected from 21-week-old individuals diagnosed as having impaired glucose tolerance (“I[#]” in Fig. 3b) in the OLETF-C group (C1, C2, C5, and C7) and as normal in the (“N[#]” in Fig. 3b) OLETF-F group (F3, F4, F5, and F6) by OGTT. Considering the disease progress in DM and that the sample volume may be sufficient for proteomic analysis, the C5, C6, and C7 individuals in the OLETF-C group and F1, F3, and F4 in the OLETF-F group were subjected for time-course investigation at following time intervals: 9, 21, 29, 37,



b

Group	Weeks of age														
	5	9	13	17	21	25	29	33	37	41	45	49	57	60	
OLETF-C	C1	N	N	N	N	I [#]	N	I	D	D	D	D	D	D	D
	C2	N	N	N	N	I [#]	D	D	D	D	D	D	D	D	D
	C3	N	N	N	I	D	D	D	D	D	D	D	D	D	D
	C4	N	N	N	I	D	I	D	D	D	D	D	D	D	D
	C5	N	N	N	I	I [#]	D	I	D	D	D	D	D	D	D
	C6	N	N	N	N	N	I	I	D	D	D	D	D	D	D
	C7	N	N	N	N	I [#]	I	I	D	D	D	D	D	D	D
OLETF-F	F1	N	N	N	N	I	D	I	D	D	I	D	D	D	D
	F2	N	N	N	N	D	D	I	D	D	D	D	D	D	D
	F3	N	N	N	N	N [#]	N	N	I	D	D	I	D	D	D
	F4	N	N	N	N	N [#]	D	I	D	D	D	D	D	D	D
	F5	N	N	N	N	N [#]	N	N	N	N	N	N	N	N	N
	F6	N	N	N	N	N [#]	I	I	I	D	D	D	D	D	D
	F7	N	N	N	N	I	I	D	D	D	D	D	D	D	D

Fig. 3. Incidence of IGT/DM and weekly results of OGTT. Oral glucose tolerance tests (OGTT) were conducted at the beginning and every 4 weeks after overnight fasting during the experiments. Based on the results of OGTT, normal glucose tolerance (N), impaired glucose tolerance (I), and diabetes (D) were classified by the definition given in the Materials and Methods. OLETF-C, OLETF rats treated with control diet; OLETF-F, OLETF rats treated with high-fiber (PHGG) diet. [#]To identify risk markers of diabetes, 4 samples of OLETF-C and 4 samples of OLETF-F (indicated by [#]) were used for proteomics analysis.

and 45 weeks of age (in F4, serum collected at 41 weeks of age was used because the amount of the corresponding sample was small).

To identify risk markers for DM, we analyzed the data in five steps as follows. Step 1) The normalized intensities of protein/peptide peaks obtained by SELDI-TOF MS were comprehensively and statistically compared between the LETO-C and OLETF-C groups. Step 2) Significant peaks obtained in step 1 were compared between the OLETF-C and OLETF-F groups. Step 3) From the significant peaks in step 2, the peaks showing risk reduction following treatment with water-soluble fiber were selected. These peaks included those that increased or decreased in peak intensities in the opposite direction as those identified in steps 1 and 2. Step 4) Artifacts (noise, multiply charged peaks, and matrix-adduct peaks) were removed from the peaks selected from step 3 and redundant peaks derived from same protein were grouped. Step 5) Time-course changes in risk marker candidates were investigated in OLETF-C and OLETF-F to evaluate the potential of the biomarkers.

By step 4, 12 specific peaks were identified as candidates of

risk markers for DM (Table 2). Fig. 6a shows the changes in the peak intensity at m/z 13,720. As shown in the boxplot (Fig. 6a), the relative peak intensity at m/z 13,720 for the OLETF rat significantly increased ($p < 0.05$) compared with those for the LETO rat at 21 weeks of age, and this increase was clearly inhibited ($p < 0.01$) by treatment by PHGG. Furthermore, Fig. 6b shows that the m/z 13,720 peak likely reflects the high-risk state for DM, particularly IGT.

Identification of protein biomarkers. Identification of the protein biomarker at m/z 13,720 was performed as follows. Fig. 7a shows the tricine SDS-PAGE pattern of fractionated from rat serum. A reducing agent such as dithiothreitol, which is used in conventional SDS-PAGE to cleave disulfide bonds in proteins, was not used because disulfide bond cleavage can induce a molecular mass shift, preventing subsequent molecular-mass confirmation. CBB-stained protein bands, which were observed at approximately 14 kDa, were comprehensively excised and subjected to passive elution; each eluted fraction was analyzed by SELDI-TOF MS. A SELDI-TOF MS spectrum of the extract of

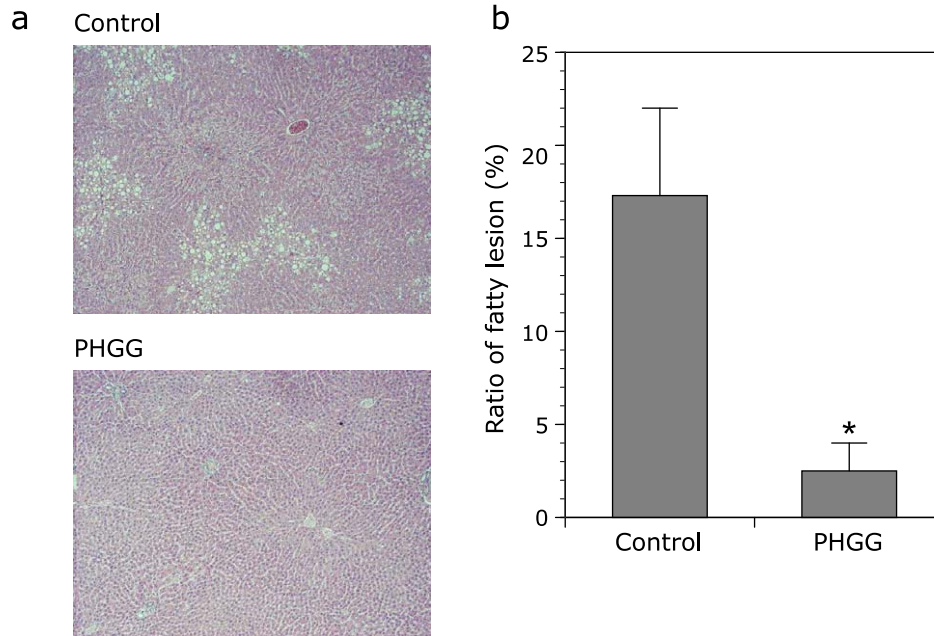


Fig. 4. Effect of PHGG on the liver fat accumulation in OLETF rats. (a) Representative microphotographs of the liver of OLETF rats. (b) Ratio of fatty lesion was evaluated using an image-analyzer. PHGG significantly suppressed liver fat accumulation in OLETF rats. The data represent the mean \pm SD ($n = 7$). * $p < 0.01$ vs the control group.

the protein band indicated by the arrow in Fig. 6a is shown in Fig. 6b. The m/z value of the dominant peak (arrowed in Fig. 7b) coincided with the target protein biomarker. The corresponding band on the replicate lane was analyzed using PMF followed by MS/MS analysis. Consequently, the m/z 13,720 peak was identified as *Rattus* transthyretin (SWISS-PROT Accession number: P02767) by sequencing four tryptic peptides using tandem MS (score = 264 using the MASCOT MS/MS ion search program; 60% coverage). However, the observed m/z value of the target protein biomarker (13,720 Da) was approximately 120 Da higher than the molecular mass value calculated from the amino acid sequence of *Rattus* transthyretin, except for the signal peptide sequence (13,598 Da). It has been reported that the single cysteine residue (Cys10) region of human transthyretin is modified with different molecules such as cysteine, homocysteine, and glutathione through disulfide bonds in the human plasma.⁽²¹⁾ We concluded that the m/z 13,720 peak was cysteinylated transthyretin based on the peak distribution around the m/z 13,720 peak in the SELDI-TOF spectra.

In addition to the m/z 13,720 peak, we attempted to identify two additional peaks (m/z 8,331 and m/z 65,700), as these peaks were potential risk markers for DM according to the results of time-course investigation. Consequently, the m/z 8,331 peak was identified as apolipoprotein C-II (gi|145553986), for which five tryptic peptides were sequenced using tandem mass spectrometry (score = 189 using the MASCOT MS/MS ion search program; 49% coverage). The m/z 8,331 peak corresponded to the molecular mass value calculated from amino acid sequence of *Rattus* apolipoprotein C-II except for the signal peptide sequence.⁽²²⁾ Finally, we succeed in identifying the other two peaks using a similar procedure. The m/z 65,700 peak was identified as serum albumin, the most abundant protein in serum.

Discussion

The present study demonstrated for the first time that chronic treatment with PHGG improved insulin resistance, delayed the onset of diabetes, and inhibited the development of diabetic

complications in OLETF rats, a model of type 2 diabetes. In our study, we performed OGTT every 4 weeks from 5 to 60 weeks of age, and classified plasma glucose levels as normal, IGTT, and diabetes based on OGTT results. Judging from the OGTT data from the early stage of experiments using rats 5 to 30 weeks of age, PHGG significantly delayed the onset of IGTT and diabetes. We also demonstrated that chronic treatment with PHGG significantly ameliorated the progression of fatty liver as well as diabetic nephropathy at 62 weeks of age of OLETF rats. Finally, we succeeded identifying serum predictive biomarker of the response to treatment with PHGG by SELDI-TOF MS.

The beneficial effects of dietary fibers on obesity in OLETF rats have been reported previously in two studies.^(23,24) Jeon *et al.*⁽²³⁾ demonstrated that treatment with fermented mushroom milk-supplemented dietary fiber for 6 weeks from 10 weeks of age prevented the onset of obesity and hypertriglyceridemia in OLETF rats. Harazaki *et al.*⁽²⁴⁾ showed that the feeding of a resistant starch diet to OLETF rats for 5 weeks from 22 weeks of age improved insulin resistance, reduced the mesenteric adipose tissue weight, and enhanced the number of small adipocytes. However, these two studies included limited data obtained from short-period treatment with dietary fibers. This is the first study to investigate the effect of chronic long-period treatment with dietary fiber on the onset of diabetes as well as on the development of diabetic complications in OLETF rats.

The OLETF rat is a good model of non-alcoholic fatty liver disease and exhibits insulin resistance, abundant visceral fat tissue, post-prandial hyperglycemia, and hepatic steatosis.⁽²⁵⁾ Many investigators have used this model to demonstrate the beneficial effects of treatment with anti-diabetic drug metformin,⁽²⁶⁾ granulocyte colony-stimulating factor,⁽²⁷⁾ nitric oxide synthase inhibition,⁽²⁸⁾ exercise training,^(3,29) and caloric restriction on hepatic stenosis.⁽³⁰⁾ It has also been reported that hepatic steatosis in OLETF rats was prevented by several food factors, including α -lipoic acid and milk thistle extracts silymarin.^(31,32) The present study clearly demonstrated that chronic long-period treatment with PHGG prevented histological hepatic steatosis. This is the first study to demonstrate a reduction of hepatic steatosis in

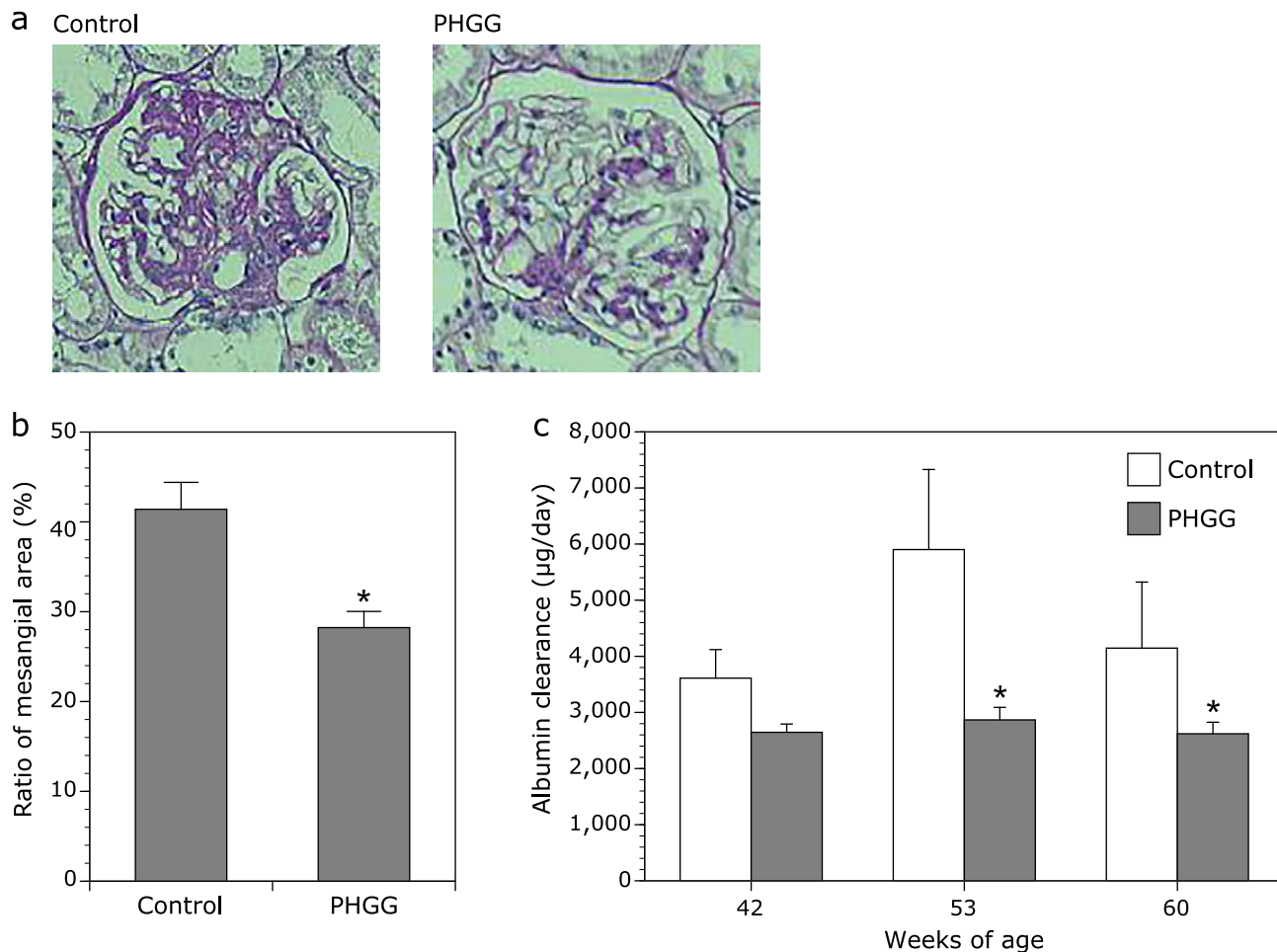


Fig. 5. Effects of PHGG on diabetic nephropathy in OLETF rats. (a) Representative microphotographs of the glomerulus of the kidney of OLETF rats. (b) Ratio of PAS-positive mesangial area (%) and (c) albumin clearance ($\mu\text{g}/\text{day}$) in OLETF rats. The data represent the mean \pm SD ($n = 7$). * $p < 0.01$ vs the control group.

Table 1. Serum biochemistry of OLETF-C and OLETF-F rats at 62 weeks of age

	OLETF-C	OLETF-F
AST (IU/L)	109 \pm 17	113 \pm 28
ALT (IU/L)	42 \pm 4.2	50 \pm 8.8
TCHO (mg/dl)	257 \pm 44	221 \pm 19
FCHO (mg/dl)	9.1 \pm 2.1	8.9 \pm 1.7
TG (mg/dl)	265 \pm 51	232 \pm 47
NEFA (mEq/L)	717 \pm 78	519 \pm 37*
CRE (mg/dl)	1.5 \pm 0.12	1.4 \pm 0.18
UN (mg/dl)	27 \pm 8.1	19 \pm 1.5
HDL (mg/dl)	171 \pm 13.5	157 \pm 6.2
LDL (mg/dl)	91 \pm 29	73 \pm 11
TBA (mg/dl)	5.7 \pm 1.3	6.5 \pm 2.6

* $p < 0.05$. AST, aspartate 2-oxoglutarate aminotransferase; ALT, alanine 2-oxoglutarate aminotransferase; TCHO, total cholesterol; FCHO, free cholesterol; TG, triglyceride; NEFA, non-esterified fatty acid; CRE, creatinine; UN, urea nitrogen; HDL, high density lipoprotein cholesterol; LDL, low density lipoprotein cholesterol; TBA, thiobarbituric acids-reactive substances.

OLETF rats by PHGG, a water-soluble dietary fiber. Although additional studies are needed to develop potential therapeutic approaches involving dietary fiber to prevent NAFLD in

humans,^(33,34) dietary interventions by PHGG may offer potential for nontoxic and physiological methods for altering the intestinal environment, leading to beneficial effects in the liver.

OLETF rats have also been used to investigate the pathophysiology of human diabetic nephropathy. Previous studies have demonstrated that the characteristic glomerular changes in diabetic nephropathy include mesangial matrix expansion, glomerular basement membrane thickening, and podocyte foot process effacement in OLETF rats. It has been reported that diabetic nephropathy in OLETF rats can be prevented by treatment with (–)-epigallocatechin 3-*O*-gallate,⁽³⁵⁾ ferulic acid,⁽³⁶⁾ granulocyte colony-stimulating factor,⁽³⁷⁾ intra-cellular delivery of anti-oxidant peptides,⁽³⁸⁾ iron restriction,⁽³⁹⁾ and taurine.⁽⁴⁰⁾ In 2005, Yokozawa *et al.*⁽⁴¹⁾ demonstrated that PHGG treatment attenuated urinary protein excretion and inhibited morphological changes in rats with streptozotocin-injected diabetic nephropathy. This is the first study to demonstrate a reduction of diabetic nephropathy in OLETF rats by PHGG, showing that treatment of OLETF rats with PHGG decreased the PAS-positive mesangial area and inhibited the increase in urinary albumin clearance compared to in control rats. The Diabetes Control and Complications Trial and some clinical studies have demonstrated that lowering high blood glucose levels prevents the development and progression of diabetic renal disease.^(42,43) In our study, blood glucose levels at fasting and at 2 h after OGTT decreased significantly in PHGG-treated OLETF rats compared to that in the control group, along

Table 2. The risk marker candidates for diabetes mellitus

Candidate No.	M/Z average	LETO-C vs OLETF-C		OLETF-C vs OLETF-F	
		p value	Change	p value	Change
1	3,497	0.021	Down	0.021	Up
2	3,559	0.021	Down	0.021	Up
3	7,026	0.083	Up	0.083	Down
4	8,331	0.083	Up	0.083	Down
5	9,060	0.021	Up	0.083	Down
6	9,255	0.021	Up	0.083	Down
7	9,446	0.021	Up	0.043	Down
8	12,792	0.021	Down	0.043	Up
9	13,720	0.021	Up	0.083	Down
10	65,700	0.083	Down	0.083	Up
11	76,750	0.021	Up	0.043	Down
12	79,085	0.021	Up	0.021	Down

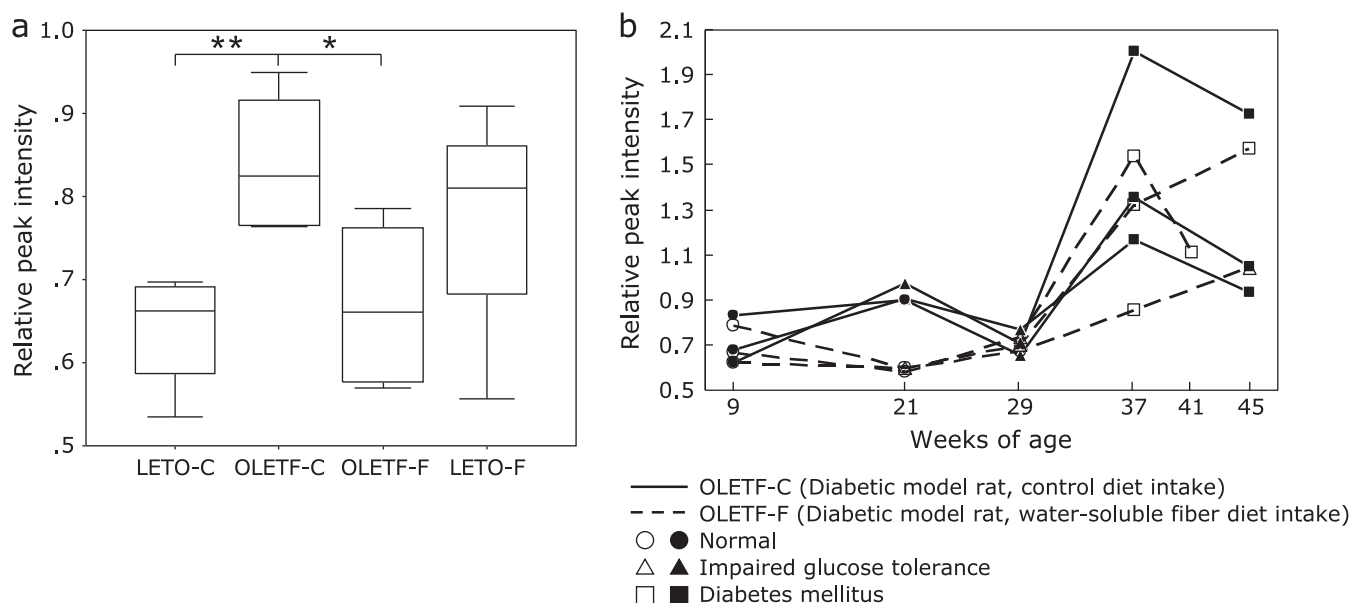


Fig. 6. Changes in peak intensity at m/z 13,720 of protein profiles obtained by SELDI-TOF MS, which were detected in the serum of 21-week-old rats. (a) Boxplot showing the difference in relative peak intensities in four groups as follows; LETO-C, OLETF-C, OLETF-F, LETO-F ($n = 4$ each group). $*p < 0.1$, $**p < 0.05$; shown with p value by Mann-Whitney U test. (b) Time-course changes in the relative peak intensity at m/z 13,720 for two groups of OLETF-C and OLETF-F ($n = 3$ each group). In the graph, the marks of data points correspond to the results of OGTT. OLETF-C, OLETF rats treated with control diet; OLETF-F, OLETF rats treated with high-fiber (PHGG) diet; LETO-C, LETO rats treated with control diet; LETO-F, LETO rats treated with high-fiber (PHGG) diet.

with increase in HOMA-IR in the PHGG treatment group. Thus, the protective effect of PHGG on diabetic nephropathy can be accomplished by lowering blood glucose levels through improved insulin secretion.

Dietary fiber intake has been inversely associated with diabetes risk, as determined in a meta-analysis of cohort studies by Schulze *et al.*⁽⁴⁴⁾ The recent European Prospective Investigation into Cancer and Nutrition (EPIC)-InterAct study showed that high intake of total fiber was associated with an 18% lower risk of incident type 2 diabetes after adjustment for life-style and dietary factors.⁽⁴⁵⁾ Because PHGG is soluble in water, has low viscosity, and is almost colorless and tasteless, properties similar to those observed for guar gum, PHGG can easily be used in sufficient amounts as dietary fiber in food; thus, PHGG has been widely used in Japan as a fiber resource since 1987 for nutritional purposes. Based on experiment data and published studies, PHGG is considered to be safe and appropriate for use as an ingredient in enteral nutrition products and liquid oral supplement products

to provide dietary fiber.⁽⁴⁶⁾ Based on results of basic experiments as well as clinical trials, the potential of PHGG in the field of preventive medicine must be further clarified, particularly regarding its role in preventing diabetes and its complications.

Protein levels in the blood reflect physiological and pathological conditions, and some proteins have been identified as biomarkers for some conditions. The development of proteomic array technology for profiling, in which a ProteinChip Array is coupled with SELDI-TOF MS, is a powerful tool for identifying new biomarkers. The advantages of this method include its speed and high-throughput capacity and that it only requires a small amount of sample. We identified fragments of apolipoprotein A1, hemopexin, and transferrin as treatment efficacy-related host factors in chronic hepatitis C using the ProteinChip Array/SELDI-TOF MS system.⁽¹⁹⁾ Aoi *et al.*⁽⁴⁷⁾ also demonstrated that apolipoproteins A-2 and C-1 and β_2 -glycoprotein-1 were altered in mice after training combined with the intake of whey protein, without significant changes induced by exercise or whey protein alone.

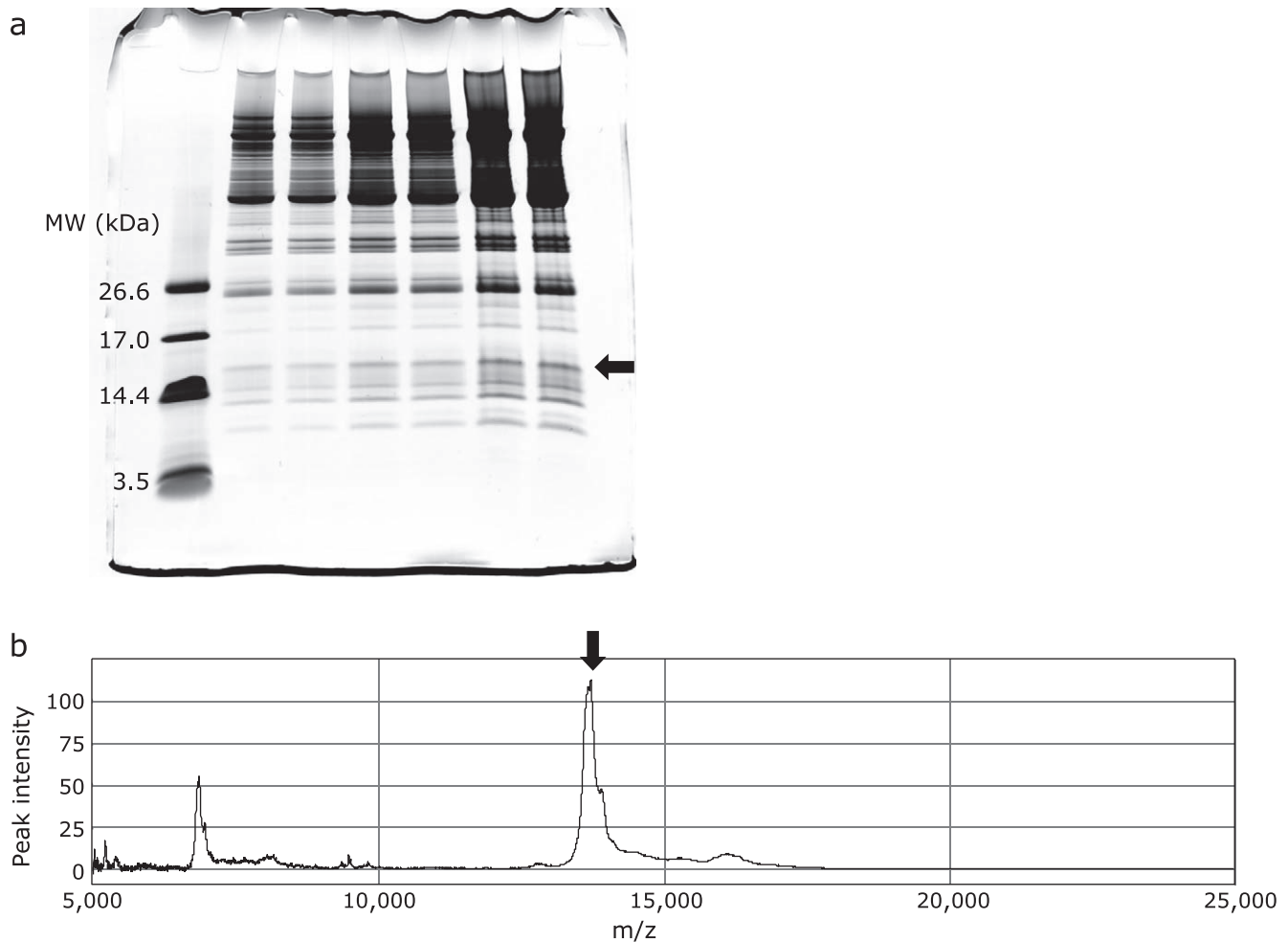


Fig. 7. Purification of the m/z 13,720 protein. (a) Normal rat serum was fractionated with HiTrap™ Q HP column and subsequently the fraction was subjected to tricine SDS-PAGE (15–20% gradient) and the gel was stained with CBB G-250. In lane 1 & 2, lane 3 & 4, and lane 5 & 6, sample was applied by 50 μ l, 100 μ l, and 200 μ l, respectively. (b) CBB-stained protein band was extracted using a passive elution procedure and the molecular mass values of the extracts were measured by SELDI-TOF MS. The arrows indicate protein bands containing the m/z 13,720 protein (a) and SELDI-TOF MS peak (b).

In the present study, we identified cysteinylated (cys)-TTR as a predictive biomarker involved in the response to treatment with PHGG on OLETF rats using the same methods. TTR has traditionally been used only as a carrier for both retinol-binding protein 4 (RBP4) and thyroxin, but also as a biomarker for nutritional status because its hepatic synthesis is mainly influenced by the adequacy of dietary protein and energy intake.⁽⁴⁸⁾ Differential levels of TTR in serum have been linked to several cancers, including breast,⁽⁴⁹⁾ ovarian,⁽⁵⁰⁾ stomach,⁽⁵¹⁾ pancreas,⁽⁵²⁾ and hepatocellular carcinomas.⁽⁵³⁾ Plasma levels of TTR, however, are also affected by acute and chronic diseases associated with an acute-phase response. Under these conditions, liver activity is concentrated on the synthesis of acute-phase response proteins, resulting in a dramatic decrease in visceral proteins. Therefore, when comparing groups of cancer patients with different stages of the disease, it is expected that plasma TTR levels are more severely affected in patients with late-stage ovarian cancer.⁽⁵⁴⁾

Five isoforms of TTR have been previously identified by MALDI analysis after immunoaffinity capture: full-length TTR, a form truncated *N*-terminally by 10 residues, and three modified isoforms, including cys-TTR, cysteinylglycylated (cysgly)-TTR, and glutathionylated (gly)-TTR.⁽⁵⁵⁾ Gericke *et al.*⁽⁵⁶⁾ reported a transient increase in cysgly-TTR in intensive care unit patients

with multiple traumas. Rüetschi *et al.*⁽⁵⁷⁾ identified cys-TTR as a cerebrospinal fluid biomarker for frontotemporal dementia. Frey *et al.*⁽⁵⁸⁾ investigated the plasma levels of these isoforms of TTR in subjects with type 2 DM by the MALDI-TOF MS and immunoprecipitation, and found no differences in the peak-height ratios of TTR isoforms and that all co-precipitated TTR isoforms were involved in binding to RBP4. These results indicate that the occurrence of TTR isoforms is not affected by the binding function of RBP4 to the TTR molecule. In the present study, we first identified cys-TTR as a predictive biomarker for the onset of diabetes as well as the progression of diabetic complications, including fatty liver and nephropathy. In addition, we recently obtained data from a preliminary clinical trial in which the plasma levels of cys-TTR significantly decreased in 4 volunteers after treatment with PHGG for 4 weeks (data not shown). The TTR protein is prone to modifications on its free cys (10) residue and thus may reflect oxidative stress. Oxidative stress and oxidative protein modification have been reported to be involved in the pathogenesis of diabetes and its complications.^(59,60) However, further studies are necessary to identify the molecular mechanism by which cys-TTR may increase in during impaired glucose tolerance.

In conclusion, we found that long-term treatment with PHGG

improved insulin resistance, delayed the onset of diabetes, and inhibited the development of diabetic complications. We also identified cys-TTR as a predictive biomarker of the response to treatment with PHGG in OLETF rats. The use of cys-TTR as a biomarker of diabetes has not been reported previously and may be used as a response-predictive biomarker in the field of preventive medicine.

Authors' Contributions

Designed the experiments and wrote the paper: YN and HI. Performed the experiments: HI, SA, KU, TT, OH. Analyzed the data: HI, SA, JM, MP, KU. Intellectual input and contributed reagents: ZY, MT, NI, TO. Overall supervision: TY. All authors read and approved the final manuscript.

Acknowledgments

This work was partially funded by Grants-in-Aid for Scientific Research (KAKENHI C) to Yuji Naito (No. 25460958) from the Japan Society for the Promotion of Science (JSPS); an Adaptable and Seamless Technology Transfer Program through target-driven R&D to Yuji Naito from the Japan Agency for Medical Research and Development (AMED).

Abbreviations

CHCA α -cyano-4-hydroxycinnamic acid

EAM	energy absorbing molecule
HOMA-IR	homeostasis model assessment of insulin resistance
HPLC	high performance liquid chromatography
LETO	Long-Evans Tokushima Otsuka
LETO-C	LETO rats fed with control standard rat diet
LETO-F	LETO rats fed with standard rat diet with 5% PHGG
MASCOT	mass values of monoisotopic peaks for searches
OGP	octyl β -D-glucopyranoside
OGTT	oral glucose tolerance test
OLETF	Otsuka Long-Evans Tokushima Fatty
OLETF-C	OLETF rats fed with control standard rat diet
OLETF-F	OLETF rats fed with standard rat diet with 5% PHGG
PAS	periodic acid-Schiff
PHGG	partially hydrolyzed guar gum
PMF	peptide mass fingerprinting
SELDI-TOF MS	surface-enhanced laser desorption/ionization time-of-flight mass spectrometry
SPA	sinapinic acid
TFA	trifluoroacetic acid

Conflict of Interest

During the last 2 years, Yuji Naito received scholarship funds from Eisai Co., Ltd., Astellas Pharma Inc., Takeda Pharmaceutical Co., Ltd., and Mitsubishi Tanabe Pharma Co., Ltd. The other authors have no conflict of interest to declare.

References

- Pathak M. Diabetes mellitus type 2 and functional foods of plant origin. *Recent Pat Biotechnol* 2014; **8**: 160–164.
- Minamiyama Y, Bito Y, Takemura S, *et al.* Calorie restriction improves cardiovascular risk factors via reduction of mitochondrial reactive oxygen species in type II diabetic rats. *J Pharmacol Exp Ther* 2007; **320**: 535–543.
- Rector RS, Thyfault JP, Morris RT, *et al.* Daily exercise increases hepatic fatty acid oxidation and prevents steatosis in Otsuka Long-Evans Tokushima Fatty rats. *Am J Physiol Gastrointest Liver Physiol* 2008; **294**: G619–G626.
- Song KH, Lee WJ, Koh JM, *et al.* alpha-Lipoic acid prevents diabetes mellitus in diabetes-prone obese rats. *Biochem Biophys Res Commun* 2005; **326**: 197–202.
- Minamiyama Y, Takemura S, Tsukioka T, *et al.* Effect of AOB, a fermented-grain food supplement, on oxidative stress in type 2 diabetic rats. *Biofactors* 2007; **30**: 91–104.
- Minamiyama Y, Takemura S, Bito Y, *et al.* Supplementation of alpha-tocopherol improves cardiovascular risk factors via the insulin signalling pathway and reduction of mitochondrial reactive oxygen species in type II diabetic rats. *Free Radic Res* 2008; **42**: 261–271.
- Takemura S, Minamiyama Y, Kodai S, *et al.* S-Allyl cysteine improves non-alcoholic fatty liver disease in type 2 diabetes Otsuka Long-Evans Tokushima Fatty rats via regulation of hepatic lipogenesis and glucose metabolism. *J Clin Biochem Nutr* 2013; **53**: 94–101.
- Kawano K, Hirashima T, Mori S, Natori T. OLETF (Otsuka Long-Evans Tokushima Fatty) rat: a new NIDDM rat strain. *Diabetes Res Clin Pract* 1994; **24 Suppl**: S317–S320.
- Chen D, Wang MW. Development and application of rodent models for type 2 diabetes. *Diabetes Obes Metab* 2005; **7**: 307–317.
- Han KQ, Huang G, Gao CF, *et al.* Identification of lung cancer patients by serum protein profiling using surface-enhanced laser desorption/ionization time-of-flight mass spectrometry. *Am J Clin Oncol* 2008; **31**: 133–139.
- Zinkin NT, Grall F, Bhaskar K, *et al.* Serum proteomics and biomarkers in hepatocellular carcinoma and chronic liver disease. *Clin Cancer Res* 2008; **14**: 470–477.
- Cheng L, Zhou L, Tao L, Zhang M, Cui J, Li Y. SELDI-TOF MS profiling of serum for detection of laryngeal squamous cell carcinoma and the progression to lymph node metastasis. *J Cancer Res Clin Oncol* 2008; **134**: 769–776.
- Wilson AM, Kimura E, Harada RK, *et al.* Beta2-microglobulin as a biomarker in peripheral arterial disease: proteomic profiling and clinical studies. *Circulation* 2007; **116**: 1396–1403.
- Wada-Isoe K, Michio K, Imamura K, *et al.* Serum proteomic profiling of dementia with Lewy bodies: diagnostic potential of SELDI-TOF MS analysis. *J Neural Transm* 2007; **114**: 1579–1583.
- Papachristou GI, Malehorn DE, Lamb J, Slivka A, Bigbee WL, Whitcomb DC. Serum proteomic patterns as a predictor of severity in acute pancreatitis. *Pancreatology* 2007; **7**: 317–324.
- Bowler RP, Ellison MC, Reisdorph N. Proteomics in pulmonary medicine. *Chest* 2006; **130**: 567–574.
- Forshed J, Pernemalm M, Tan CS, *et al.* Proteomic data analysis workflow for discovery of candidate biomarker peaks predictive of clinical outcome for patients with acute myeloid leukemia. *J Proteome Res* 2008; **7**: 2332–2341.
- Trocme C, Marotte H, Baillet A, *et al.* Apolipoprotein A-I and platelet factor 4 are biomarkers for infliximab response in rheumatoid arthritis. *Ann Rheum Dis* 2009; **68**: 1328–1333.
- Fujita N, Nakanishi M, Mukai J, *et al.* Identification of treatment efficacy-related host factors in chronic hepatitis C by ProteinChip serum analysis. *Mol Med* 2011; **17**: 70–78.
- Shevchenko A, Wilm M, Vorm O, Mann M. Mass spectrometric sequencing of proteins silver-stained polyacrylamide gels. *Anal Chem* 1996; **68**: 850–858.
- Lim A, Sengupta S, McComb ME, *et al.* *In vitro* and *in vivo* interactions of homocysteine with human plasma transthyretin. *J Biol Chem* 2003; **278**: 49707–49713.
- Andersson Y, Thelander L, Bengtsson-Olivecrona G. Rat apolipoprotein C-II lacks the conserved site for proteolytic cleavage of the pro-form. *J Lipid Res* 1991; **32**: 1805–1809.
- Jeon BS, Park JW, Kim BK, *et al.* Fermented mushroom milk-supplemented dietary fibre prevents the onset of obesity and hypertriglyceridaemia in Otsuka Long-Evans Tokushima fatty rats. *Diabetes Obes Metab* 2005; **7**: 709–715.
- Harazaki T, Inoue S, Imai C, Mochizuki K, Goda T. Resistant starch improves insulin resistance and reduces adipose tissue weight and CD11c expression in rat OLETF adipose tissue. *Nutrition* 2014; **30**: 590–595.
- Song YS, Fang CH, So BI, *et al.* Time course of the development of non-alcoholic fatty liver disease in the Otsuka long-evans Tokushima Fatty rat. *Gastroenterol Res Pract* 2013; **2013**: 342648.
- Linden MA, Fletcher JA, Morris EM, *et al.* Combining metformin and aerobic exercise training in the treatment of type 2 diabetes and NAFLD in OLETF rats. *Am J Physiol Endocrinol Metab* 2014; **306**: E300–E310.

- 27 Song YS, Fang CH, So BI, Park JY, Jun DW, Kim KS. Therapeutic effects of granulocyte-colony stimulating factor on non-alcoholic hepatic steatosis in the rat. *Ann Hepatol* 2013; **12**: 115–122.
- 28 Sheldon RD, Padilla J, Jenkins NT, Laughlin MH, Rector RS. Chronic NOS inhibition accelerates NAFLD progression in an obese rat model. *Am J Physiol Gastrointest Liver Physiol* 2015; **308**: G540–G549.
- 29 Linden MA, Fletcher JA, Morris EM, *et al.* Treating NAFLD in OLETF rats with vigorous-intensity interval exercise training. *Med Sci Sports Exerc* 2015; **47**: 556–567.
- 30 Rector RS, Uptergrove GM, Morris EM, *et al.* Daily exercise vs. caloric restriction for prevention of nonalcoholic fatty liver disease in the OLETF rat model. *Am J Physiol Gastrointest Liver Physiol* 2011; **300**: G874–G883.
- 31 Jung TS, Kim SK, Shin HJ, Jeon BT, Hahm JR, Roh GS. α -lipoic acid prevents non-alcoholic fatty liver disease in OLETF rats. *Liver Int* 2012; **32**: 1565–1573.
- 32 Kim M, Yang SG, Kim JM, Lee JW, Kim YS, Lee JI. Silymarin suppresses hepatic stellate cell activation in a dietary rat model of non-alcoholic steatohepatitis: analysis of isolated hepatic stellate cells. *Int J Mol Med* 2012; **30**: 473–479.
- 33 Yang M, Gong S, Ye SQ, *et al.* Non-alcoholic fatty liver disease in children: focus on nutritional interventions. *Nutrients* 2014; **6**: 4691–4705.
- 34 Ma J, Fox CS, Jacques PF, *et al.* Sugar-sweetened beverage, diet soda, and fatty liver disease in the Framingham Heart Study cohorts. *J Hepatol* 2015; **63**: 462–469.
- 35 Yamabe N, Yokozawa T, Oya T, Kim M. Therapeutic potential of (–)-epigallocatechin 3-O-gallate on renal damage in diabetic nephropathy model rats. *J Pharmacol Exp Ther* 2006; **319**: 228–236.
- 36 Choi R, Kim BH, Naowaboot J, *et al.* Effects of ferulic acid on diabetic nephropathy in a rat model of type 2 diabetes. *Exp Mol Med* 2011; **43**: 676–683.
- 37 So BI, Song YS, Fang CH, *et al.* G-CSF prevents progression of diabetic nephropathy in rat. *PLoS One* 2013; **8**: e77048.
- 38 Park Y, Kim H, Park L, *et al.* Effective delivery of endogenous antioxidants ameliorates diabetic nephropathy. *PLoS One* 2015; **10**: e0130815.
- 39 Matsumoto M, Sasaki N, Tsujino T, Akahori H, Naito Y, Masuyama T. Iron restriction prevents diabetic nephropathy in Otsuka Long-Evans Tokushima fatty rat. *Ren Fail* 2013; **35**: 1156–1162.
- 40 Koh JH, Lee ES, Hyun M, *et al.* Taurine alleviates the progression of diabetic nephropathy in type 2 diabetic rat model. *Int J Endocrinol* 2014; **2014**: 397307.
- 41 Yokozawa T, Nakagawa T, Oya T, Okubo T, Juneja LR. Green tea polyphenols and dietary fibre protect against kidney damage in rats with diabetic nephropathy. *J Pharm Pharmacol* 2005; **57**: 773–780.
- 42 The Diabetes. The effect of intensive treatment of diabetes on the development and progression of long-term complications in insulin-dependent diabetes mellitus. *N Engl J Med* 1993; **329**: 977–986.
- 43 UK Prospective. Intensive blood-glucose control with sulphonylureas or insulin compared with conventional treatment and risk of complications in patients with type 2 diabetes (UKPDS 33). *Lancet* 1998; **352**: 837–853.
- 44 Schulze MB, Schulz M, Heidemann C, Schienkiewitz A, Hoffmann K, Boeing H. Fiber and magnesium intake and incidence of type 2 diabetes: a prospective study and meta-analysis. *Arch Intern Med* 2007; **167**: 956–965.
- 45 InterAct Consortium. Dietary fibre and incidence of type 2 diabetes in eight European countries: the EPIC-InterAct Study and a meta-analysis of prospective studies. *Diabetologia* 2015; **58**: 1394–1408.
- 46 Yoon SJ, Chu DC, Juneja LR. Chemical and physical properties, safety and application of partially hydrolyzed guar gum as dietary fiber. *J Clin Biochem Nutr* 2008; **42**: 1–7.
- 47 Aoi W, Takanami Y, Kawai Y, *et al.* Dietary whey hydrolysate with exercise alters the plasma protein profile: a comprehensive protein analysis. *Nutrition* 2011; **27**: 687–692.
- 48 Ingenbleek Y, Young V. Transthyretin (prealbumin) in health and disease: nutritional implications. *Annu Rev Nutr* 1994; **14**: 495–533.
- 49 Chung L, Moore K, Phillips L, Boyle FM, Marsh DJ, Baxter RC. Novel serum protein biomarker panel revealed by mass spectrometry and its prognostic value in breast cancer. *Breast Cancer Res* 2014; **16**: R63.
- 50 Zhang Z, Bast RC Jr, Yu Y, *et al.* Three biomarkers identified from serum proteomic analysis for the detection of early stage ovarian cancer. *Cancer Res* 2004; **64**: 5882–5890.
- 51 Ahn HS, Shin YS, Park PJ, *et al.* Serum biomarker panels for the diagnosis of gastric adenocarcinoma. *Br J Cancer* 2012; **106**: 733–739.
- 52 Felix K, Hauck O, Fritz S, *et al.* Serum protein signatures differentiating autoimmune pancreatitis versus pancreatic cancer. *PLoS One* 2013; **8**: e82755.
- 53 Sarvari J, Mojtahedi Z, Kuramitsu Y, *et al.* Comparative proteomics of sera from HCC patients with different origins. *Hepat Mon* 2014; **14**: e13103.
- 54 Schweigert FJ, Sehoul J. Transthyretin, a biomarker for nutritional status and ovarian cancer. *Cancer Res* 2005; **65**: 1114.
- 55 Brauer HA, Lampe PD, Yasui YY, Hamajima N, Stolz ML. Biochips that sequentially capture and focus antigens for immunoaffinity MALDI-TOF MS: a new tool for biomarker verification. *Proteomics* 2010; **10**: 3922–3927.
- 56 Gericke B, Raila J, Deja M, *et al.* Alteration of transthyretin microheterogeneity in serum of multiple trauma patients. *Biomark Insights* 2007; **2**: 299–306.
- 57 Rüetschi U, Zetterberg H, Podust VN, *et al.* Identification of CSF biomarkers for frontotemporal dementia using SELDI-TOF. *Exp Neurol* 2005; **196**: 273–281.
- 58 Frey SK, Spranger J, Henze A, Pfeiffer AF, Schweigert FJ, Raila J. Factors that influence retinol-binding protein 4-transthyretin interaction are not altered in overweight subjects and overweight subjects with type 2 diabetes mellitus. *Metabolism* 2009; **58**: 1386–1392.
- 59 Maiese K. New insights for oxidative stress and diabetes mellitus. *Oxid Med Cell Longev* 2015; **2015**: 875961.
- 60 Nowotny K, Jung T, Hohn A, Weber D, Grune T. Advanced glycation end products and oxidative stress in type 2 diabetes mellitus. *Biomolecules* 2015; **5**: 194–222.